Magnetic Resonance Imaging of Innervational and Extraocular Muscle Abnormalities in Duane-Radial Ray Syndrome

Joseph L. Demer,[1,2,3,4] *Robert A. Clark,*[1] *Key Hwan Lim,*[1,5] *and Elizabeth C. Engle*[6,7]

Purpose. The authors used magnetic resonance imaging (MRI) to study extraocular muscles (EOMs) and nerves in Duane-radial ray (Okihiro) syndrome (DRRS) caused by mutations in the transcription factor *SALL4*.

Methods. The authors examined four male and two female affected members of a pedigree previously reported to cosegregate DRRS and a heterozygous *SALL4* mutation. Coronal T1-weighted magnetic resonance images of the orbits and heavily T2-weighted images in the plane of the cranial nerves were obtained in four subjects. MRI findings were correlated with motility examinations and published norms obtained using identical technique.

Results. Five of the six subjects with DRRS had radial ray abnormalities including thumb, radial artery, radial bone, and pectoral muscle hypoplasia. Three had bilateral and three had unilateral ocular involvement. Seven eyes had limitation of both abduction and adduction, whereas two had limitations only of abduction. Most affected eyes had lid fissure narrowing and retraction in adduction. Intraorbital and intracranial abducens nerves (CN6) were small to absent, particularly ipsilateral to abduction deficiency. All subjects undergoing MRI had normal intracranial oculomotor nerves (CN3). Optic nerve (ON) cross-section findings were similar to normal. EOMs and pulleys were structurally normal in most subjects. In some affected orbits, a branch of CN3 closely approximated and presumably innervated the LR.

Conclusions. DRRS encompasses a Duane syndrome phenotype, with a variable and asymmetric endophenotype including marked CN6 hypoplasia and probable innervation or coinnervation of the LR by CN3. This endophenotype is more limited than reported in DURS2-linked Duane syndrome (On-line Mendelian Inheritance in Man, OMIM 604356) and CFEOM1 (OMIM 135700), which are clinically similar congenital cranial dysinnervation disorders that also feature CN3 hypoplasia and more widespread EOM abnormalities. (*Invest Ophthalmol Vis Sci.* 2007;48:5505–5511) DOI:10.1167/iovs.07-0772

Duane retraction syndrome (DRS) is characterized by congenital horizontal duction deficit, narrowing of the palpebral fissure on adduction, and globe retraction with occasional upshoot or downshoot in adduction.[1] Innervation of the lateral rectus (LR) by the abducens nerve (CN6) is deficient in both DRS and CN6 palsy. Unlike CN6 palsy, however, eyes in central gaze are frequently aligned in DRS.[2] This evidence for contractile tonus in the LR suggests that the involved LR either is solely innervated or is coinnervated by a branch of the oculomotor nerve (CN3). Early electrophysiological studies of sporadic DRS suggested the absence of normal CN6 innervation to the LR muscle as the cause of DRS, with paradoxical LR innervation in adduction.[3,4] Absence of the CN6 nerve and motor neurons with LR innervation by an aberrant CN3 branch has been confirmed by autopsy in one subject with sporadic unilateral[5] and another with sporadic bilateral DRS.[6] Parsa et al.[7] first used magnetic resonance imaging (MRI) to demonstrate the absence of the subarachnoid CN6 in sporadic DRS, a finding confirmed in some, but not all, sporadic and familial occurrences.[8–11]

Although many DRS occurrences appear sporadic, the less common inherited forms can provide molecular genetic and phenotypic insights. Isolated DRS can segregate as a dominant trait in large pedigrees and has been linked to chromosome 2 (DURS2 locus, On-line Mendelian Inheritance in Man [OMIM] 604356).[12–14] High-resolution MRI in affected members of DURS2-linked DRS pedigrees (DURS2) revealed small to undetectable CN6 and provided direct evidence of LR innervation by CN3, as well as optic nerve abnormalities.[11] These MRI studies indicate that the endophenotype—the internal phenotype of the structure and function of EOMs—may be complex and variable, not reflective of seemingly similar external findings in subjects with DRS. The *DURS2* gene has not yet been identified.

The present study was performed to characterize the endophenotype in a family with Duane-radial ray syndrome (DRRS; also known as Okihiro syndrome; OMIM 607323). DRRS is the dominant association of unilateral or bilateral DRS with unilateral or bilateral dysplasia of the radial bone, artery, and thumb and can result from heterozygous mutations in *SALL4*, a zinc finger transcription factor.[15,16] The developmental expression profile and functional role of *SALL4* in normal and abnormal ocular motor development have not yet been elucidated, and *SALL4* mutations have not been identified in persons with isolated sporadic DRS.[17]

Methods

Subjects and Clinical Examination

Six affected members of a single pedigree previously reported to harbor a *SALL4* single base-pair deletion, 1904delT (Pedigree V[15]), agreed to undergo clinical examinations and MRI after giving written informed consent to a protocol conforming to the Declaration of Helsinki and approved by relevant institutional review boards. Subjects

From the [1]Department of Ophthalmology and Jules Stein Eye Institute, and Departments of [2]Neurology, [3]Bioengineering, and [4]Neuroscience Interdepartmental Programs, University of California, Los Angeles, California; the [5]Department of Ophthalmology, College of Medicine, Ewha Womans University, Seoul, Korea; [6]Programs in Genomics and Department of Neurology, Children's Hospital, Boston, Massachusetts; and the [7]Department of Neurology, Harvard Medical School, Boston, Massachusetts.

Supported by United States Public Health Service National Eye Institute Grants EY13583, EY08313, and EY00331. JLD is Leonard Apt Professor of Ophthalmology.

Submitted for publication June 21, 2007; revised August 15, 2007; accepted October 8, 2007.

Disclosure: **J.L. Demer**, None; **R.A. Clark**, None; **K.H. Lim**, None; **E.C. Engle**, None

The publication costs of this article were defrayed in part by page charge payment. This article must therefore be marked "*advertisement*" in accordance with 18 U.S.C. §1734 solely to indicate this fact.

Corresponding author: Joseph L. Demer, Department of Ophthalmology, Jules Stein Eye Institute, 100 Stein Plaza, UCLA, Los Angeles, CA 90095-7002; jld@ucla.edu.

underwent examination of corrected visual acuity, ocular motility, eyelid structure and function, binocular alignment, anterior segment anatomy, and ophthalmoscopy. Ophthalmic histories were obtained, with corroboration of previous ocular surgeries from operative records where possible.

Magnetic Resonance Imaging

MRI was performed with a 1.5 T scanner (General Electric Signa; Milwaukee, WI) in four subjects. Subject 1 is a child who was unable to undergo MRI because of metallic dental braces, and subject 4 had a claustrophobic reaction before MRI could be conducted. Orbital imaging was performed as described elsewhere in detail.[18–22] Imaging posterior to the orbital apex in some subjects was performed using the standard head coil. When surface coils were used, images of 2-mm thickness in a matrix of 256 × 256 were obtained over a field of view of 6 to 8 cm for a resolution in plane of 234 to 312 μm. Imaging of subarachnoid cranial nerves was performed in 1-mm thick image planes using the heavily T2-weighted FIESTA sequence.[23,24] In-plane resolution was 195 μm over a 10-cm field of view (matrix, 512 × 512) with 10 excitations.

Digital MRI images were quantified using the programs NIH Image 1.59 and ImageJ 1.33μ software (ver. 1.30; available by ftp at http://rsb.info.nih.gov/nih-image; developed by Wayne Rasband, National Institutes of Health, Bethesda, MD). In coronal planes, each rectus EOM was described by the "area centroid" using methods previously described.[25] Cross-sectional areas were determined using ImageJ, which, because of a difference in perimeter treatment, produces different area values than NIH Image. Centroid determinations did not differ between NIH Image and ImageJ. The globe center was determined.[20] Coronal plane pulley locations were determined from the EOM centroids at published anteroposterior positions.[20] Inferior oblique (IO) muscles were analyzed using outlined cross-sections in quasi-sagittal images.[26] Optic nerve cross-sections were analyzed in the first image plane immediately posterior to the globe.[27]

We computed rectus EOM volumes by summing the cross-sections for each EOM in the image plane containing the junction of the globe and optic nerve and the next five contiguous image planes posterior to this plane and then multiplying by the image plane thickness of 2 mm. Although this approach fails to account for EOM volume deep to the image planes collected, the technique was identical with that used for published data in control subjects and subjects with CFEOM1[24] and DURS2,[11] and it avoided the confounding problem of defining the borders of highly dysplastic deep portions of EOMs.

Results

Clinical Findings in DRRS

General characteristics of the subjects are summarized in Table 1. Mean corrected visual acuity was identical in left and right eyes of affected subjects (Table 1) and averaged −0.02 logMAR ($20/20^{+}$ Snellen). The maximum interocular acuity difference observed was 0.45 logMAR, found in subject 6, indicating minimal to no amblyopia.

Subjects exhibited a variable and often asymmetrical pattern of abnormalities of the radial bone, radial artery, and thumb, as detailed in Figure 1 and Table 1. Subject 2 had, in addition, hypoplasia of the left pectoral musculature.

Subjects 2, 3, and 6 exhibited unilateral ocular motility abnormalities. Subject 1 exhibited asymmetrical bilateral DRS, and subjects 4 and 5 exhibited symmetrical bilateral DRS. Posterior globe displacement, termed retraction, was evident on attempted adduction of all affected eyes except those of subjects 3 and 4, in whom this finding could not be ascertained with certainty. Horizontal saccades were slowed in the direction of limited duction in affected eyes and appeared normal in unaffected directions and unaffected eyes. Vertical saccades were examined in all subjects except subject 2, in whom this was omitted because of time considerations. Vertical saccades were normal in all examined subjects except for subject 4, who was unable to make vertical saccades but who had a normal range of vertical slow phases during vestibular stimulation by the doll's head maneuver. Subject 4 had almost complete horizontal ophthalmoplegia, even to the horizontal doll's head maneuver, but had some convergence. No subject exhibited blepharoptosis. Subjects 1 and 5 had previously undergone surgery for strabismus correction before the study. The remaining subjects had not previously undergone ocular surgery.

The common clinical classification by Huber of DRS consists of three groups: type 1, with limitation of abduction only; type 2, with limitation of adduction only; and type 3, with limitation of both abduction and adduction.[3,28] This classification is interpreted here with respect to duction along the horizontal meridian given that the limitation in several subjects varied markedly with vertical eye position. As noted in Table 1, five right and two left eyes were classified as DRS type 3, whereas two left eyes exhibited DRS type 1. Subject 1 exhibited DRS type 3 in the right eye and type 1 in the left eye, with

Table 1. Subject Characteristics

Subject	Age (y)	Sex	Absent Radial Pulses		Thenar Hypoplasia		Corrected Visual Acuity†		Horizontal Alignment	DRS Type*		MRI
			R	L	R	L	R	L		R	L	
1	13	M	+	+	+	+	−0.05	0.05	A-ET	3	1	No
2	42	M	+	+	+	+	−0.10	−0.20	ET	3	−	Yes
3	46	M	−	−	−	−	−0.05	−0.05	ET	−	1	Yes
4	45	F	+	−	+	+	−0.05	−0.05	Orthotropic, limited vertical versions	3	3	No
5	45	M	+	+	+	+	−0.10	0.05	V-XT	3	3	Yes
6	68	F	−	−	+	+	0.40	−0.05	Orthotropic	3	−	Yes
Mean	45	NA	NA	NA	NA	NA	0.01	−0.04	NA	NA	NA	NA
SEM	8	NA	NA	NA	NA	NA	0.02	0.03	NA	NA	NA	NA

+, finding present; −, finding absent; ET, esotropia; A-ET, "A" pattern esotropia; V-XT, "V" pattern exotropia; NA, not applicable.

* Clinical classification of Huber: type 1, limitation of abduction only; type 2, limitation of adduction only; type 3, limitation of abduction and adduction.[3,28]

† logMAR.

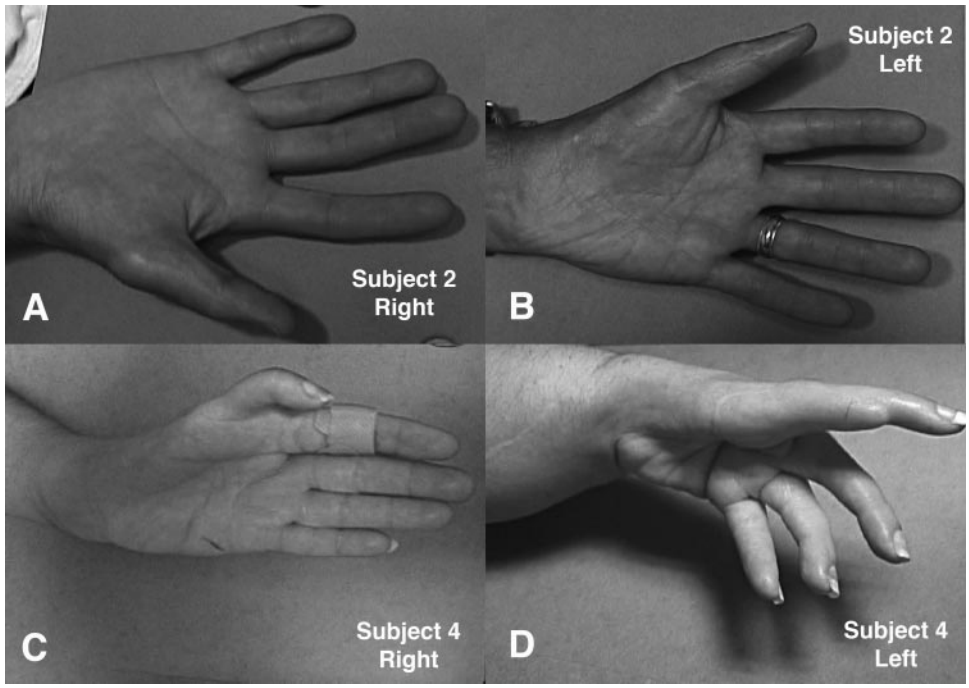

FIGURE 1. Spectrum of hand abnormalities in Duane-radial ray syndrome. (**A**, **B**) Subject 2 exhibits asymmetrical hypoplasia of the left thumb and thenar eminence. (**C**, **D**) Subject 4 exhibits absence of the left thumb and radial bone and has undergone surgical reconstruction of the right thumb.

the left eye also exhibiting limited supraduction (Fig. 2). Subjects 4 and 5 had bilateral type 3 DRS.

As indicated in Table 1, three affected subjects exhibited esotropia in central gaze, and one exhibited exotropia. The strabismus was unaltered (concomitant) during vertical gaze changes in subjects 2 and 3 only but varied with vertical gaze in subjects 1 and 5. Subject 1 had incomitant horizontal strabismus evocative of the letter *A* or the Greek letter λ because the eyes were in a more divergent position in down gaze than in upgaze. Subject 5 had exotropia that increased in upward gaze.

Orbital Imaging Findings in DRRS

Structural abnormalities of EOMS were not severe or common among subjects with DRRS. Only subject 5 had splitting of the deep portion of the right LR and hypoplasia of the deep portion of the left LR (Fig. 3). EOMs were structurally normal in the remaining subjects who underwent MRI.

Quantitative Analysis of Rectus EOMs

Despite previous strabismus surgery, orbital MRI reasonably reflects the sizes and positions of EOM bellies because surgery is largely confined to the region of the insertional tendons.[11] Mean volumes of each of the four rectus EOMs in the six contiguous image planes, including and posterior to the junction of the globe and optic nerve, were not significantly different from normal when both orbits of each subject were included ($P > 0.05$; Table 2). The volume measurement did not, however, incorporate rectus EOMs in their most apical portions. Mean rectus EOM volumes in DRRS were also not signif-

FIGURE 2. Subject 1 exhibited DRRS type 3 in the right eye and type 1 in the left eye. Note limited abduction and adduction of the right eye, upshot of the right eye in adduction, and narrowing of the right palpebral fissure in adduction. Note limited abduction and supraduction of the left eye. There was palpebral fissure narrowing and globe retraction in adduction bilaterally. Eyelids were manually elevated in the lower row only because the lids would otherwise have covered the eyes.

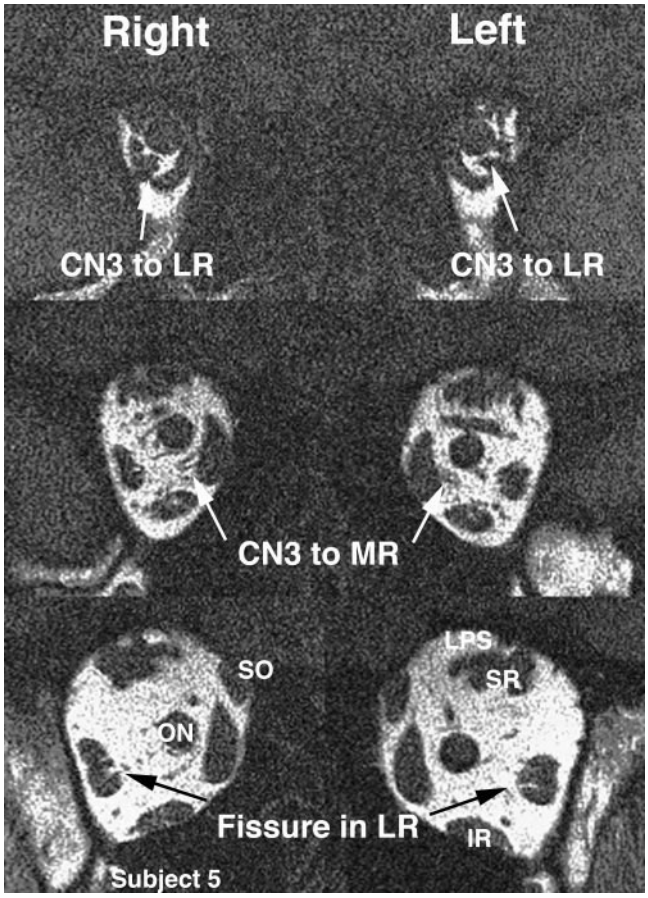

FIGURE 3. MRI of orbits of subject 5, who exhibited bilateral type 3 DRS. Of the subjects with DRS, subject 5 had the most severe EOM abnormalities consisting of mild longitudinal fissuring of the LR muscles and hypoplasia of the deep portion of the left LR. Image planes 2-mm thick, skipping planes between those illustrated. CN3, inferior division of oculomotor nerve; IR, inferior rectus muscle; LPS, levator palpebrae superioris muscle; MR, medial rectus muscle; ON, optic nerve; SO, superior oblique muscle; SR, superior rectus muscle.

icantly different from those previously reported in DURS2.[11] A similar analysis limited to orbits affected by DRS also showed no significant differences from normal.

Quantitative Analysis of Oblique EOMs

Previously reported control IO volume averages 301 ± 11 μL (N = 55).[11] Quasi-sagittal imaging was performed in subjects 2, 3, and 6. Considering both eyes of these subjects, mean IO volume was 251 ± 25 μL, which was not significantly different from normal. However, subjects 2 and 3 had subnormal IO volumes of 160 to 186 μL, offset by above normal volumes in subject 6 of 353 and 450 μL.

For comparability to the published literature, SO size was assessed by maximal cross-section in quasi-coronal image planes. Considering both eyes of the 10 normal subjects previously reported,[11] mean maximal SO cross-section was 22.0 ± 0.9 (SEM) mm^2. After averaging both eyes of the four subjects with DRRS who underwent imaging, the mean maximal SO cross-section was not significantly different from normal at 24.5 ± 0.9 mm^2.

Rectus Muscle Paths

EOMs pass through their connective tissue pulleys such that the anterior locations of these paths indicate the respective pulley locations in the coronal plane.[22] Because subjects with DRRS were typically unable to achieve eccentric gaze positions, no inflections in rectus EOM paths were present to identify the anteroposterior coordinates of the rectus pulleys. Therefore, it was assumed the rectus pulley anteroposterior coordinates were the same as those known for unaffected subjects.[22] This was considered reasonable because variations in anteroposterior coordinates would minimally influence horizontal and vertical pulley coordinates. The coordinates of rectus pulleys in DRRS did not differ significantly from normal ($P > 0.005$), except for 3- to 4-mm lateral displacement of the superior rectus (SR) attributed entirely to subjects 2 and 5, who were the only subjects to exhibit the displacement.

Imaging of Intraorbital Motor Nerves

It was possible to examine in the deep orbit the motor nerves to the EOMs in image planes of 1.5- to 2-mm thickness and a field of view of 6–8 cm. Normal intraorbital motor nerves to individual EOMs are represented by one or at most a few pixels in the coronal image planes used here; images of intraorbital motor nerves are insufficiently precise for quantitative analysis of motor nerve size. However, qualitative impressions were consistently obtained and are illustrated here. Assessments were confirmed by evaluation of multiple contiguous MRI planes to trace the paths of presumed nerves to their target EOMs.

The intraorbital CN6 was absent or below detection in the right orbit of subjects 2 and 6, each of whom exhibited right DRS type 3. The intraorbital CN6 was absent or below detection in the left orbit of subject 3, who exhibited left DRS type 1. Subject 5 had an identifiable CN6 in each orbit and exhibited DRS type 3. In the right orbit of subjects 5 and 6 and in the left orbit of subject 3, a branch of CN3 was in close contact with the inferior belly of the LR (Fig. 3). The intimate contact of the inferior division of CN3 with the LR suggested that the CN3 branch entered the EOM, though the limited resolution of MRI precludes confirmation of actual innervation at the level of EOM fibers. The medial rectus and inferior rectus muscles were innervated by CN3 branches in all orbits imaged, though in subjects 2 and 3 these motor nerves appeared of subnormal size.

Imaging of Intracranial Motor Nerves

Heavily T_2-weighted imaging of the skull base region was conducted in 1-mm thick slices at 195 μm resolution in the plane of the optic chiasm and major cranial nerves to the orbit. This technique has just sufficient resolution to consistently

TABLE 2. Muscle Volumes in Subjects with DRRS and DURS2-Linked DRS[11]

	Control Subjects (n = 9)		Subjects with DRRS (n = 4)		Subjects with DURS2 (n = 7)	
Muscle	**Mean**	**SEM**	**Mean**	**SEM**	**Mean**	**SEM**
Medial rectus	395	16	401	28	376	12
Superior rectus	370	32	411	26	374	16
Lateral rectus	428	15	460	47	385	17
Inferior rectus	385	12	429	20	387	15

Data are expressed as volume (mm^3). Subjects contributed data from both orbits where available. Volumes for rectus EOMs included contributions from six contiguous image planes extending posteriorly beginning at the globe-optic nerve junction. There were no significant differences among the three groups ($P > 0.05$).

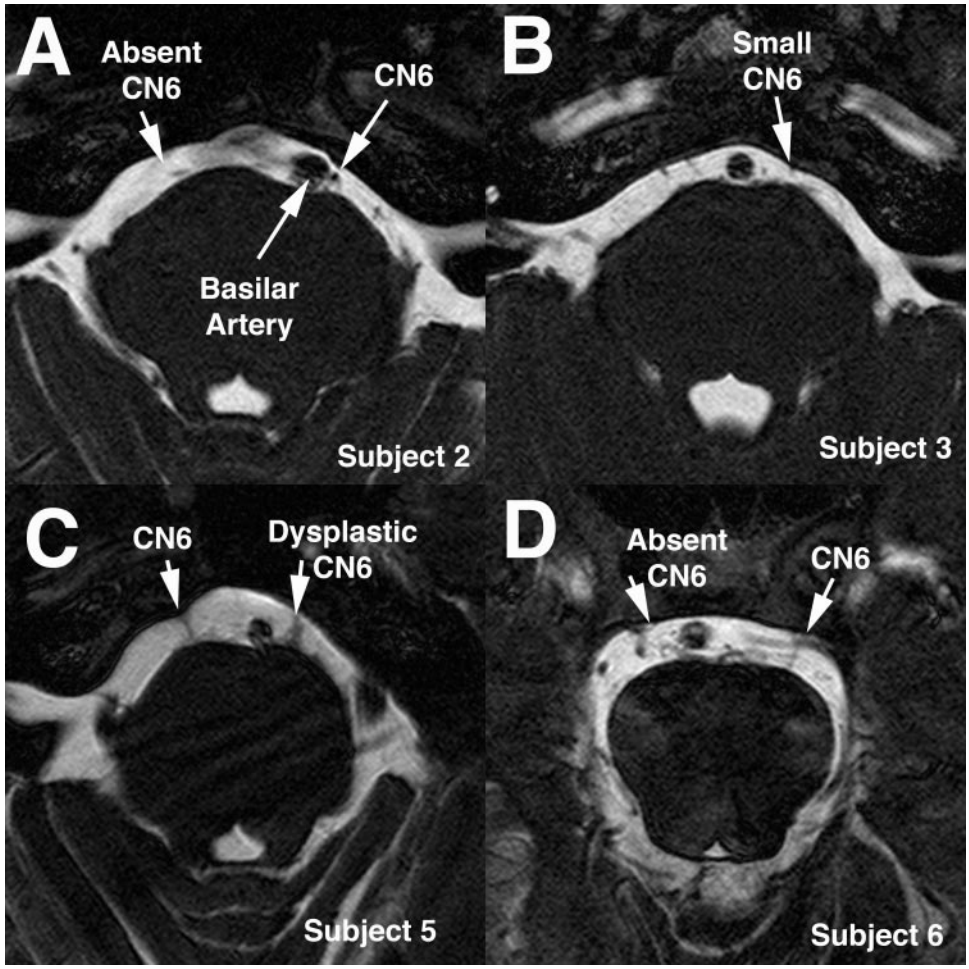

FIGURE 4. Heavily T2-weighted MRI of the pons and subarachnoid portion of the abducens nerve (CN6) in subjects with DRRS. Images are 1-mm thick, parallel to the plane of the optic chiasm, and were chosen from sets of contiguous image planes. Note unilateral absence of CN6 in subjects 2 and 6, hypoplasia of left CN6 in subject 3, and dysplasia of CN6 in subject 5.

demonstrate normal subarachnoid CN6s, whereas it consistently demonstrates the larger CN3s of normal subjects.[11,24]

The right subarachnoid CN6 was not demonstrable in subjects 2 and 6 (Fig. 4). In subject 3, the left subarachnoid CN6 appeared smaller than the right, whereas in subject 5 the right CN6 appeared smaller than the left and the left appeared dysplastic (Fig. 4). The CN3 was present in all subjects with DRRS who underwent imaging. Averaged bilaterally, CN3 width was 1.91 ± 0.13 mm (mean ± SEM) in affected subjects, not significantly different from the width of 2.10 ± 0.07 mm for normal subjects.[29]

Optic Nerve

Given that ON cross-section normally decreases from anterior to posterior in the orbit as a result of the reduction of connective tissues surrounding the axon bundles,[27] ON cross-sections were analyzed at the 2-mm-thick image plane closest to the globe-optic nerve junction. Mean (± SEM) cross-section of the optic nerve in eight orbits with DRRS was 8.90 ± 0.44 mm^2, not significantly different from normal. The ON also appeared ophthalmoscopically normal in all subjects.

DISCUSSION

Definition of the DRRS Endophenotype

As this and previous published pedigrees demonstrate, different affected family members harboring the same *SALL4* mutation can exhibit unilateral or bilateral DRS of type 1 or 3.[15] This suggests that additional genetic or environmental factors modulate the phenotype in DRRS.

MRI in the four DRRS family members revealed a spectrum of CN6 endophenotypes: undetectable both intracranially and intraorbitally on the affected side in subjects 2 and 6; detectable intracranially but not intraorbitally on the affected side in subject 3; and detected in intracranially and intraorbitally on both affected sides in subject 5. Although the subarachnoid CN6 was visualized unilaterally in subject 3 and bilaterally in subject 5, it appeared small or dysplastic in each. In addition, in two of three affected orbits without CN6 and in one of two affected orbits with CN6, CN3 appeared to innervate or coinnervate the LR.

These MRI findings in DRRS confirm limited autopsy[5,6] and electromyographic[3,4,30] reports of CN6 aplasia with LR misinnervation by CN3 in DRS. In addition, MRI evidence of absence or marked hypoplasia of the subarachnoid CN6 appears to occur in DRRS at approximately the same frequency as in DURS2.[11] These findings are in accordance with previous MRI reports of occasional absence of the subarachnoid CN6 in sporadic DRS. Kim and Hwang have emphasized the frequent absence of CN6 ipsilateral to DRS type 1[10,31] and type 3[10] but the presence of CN3 ipsilateral to type 2.[10]

The ophthalmic phenotype and the CN6 endophenotype of DRRS resemble those previously reported for DURS2, except for more frequent A or λ strabismus patterns in the latter. The endophenotype of DRRS, however, is otherwise distinct from both DURS2 and from CFEOM1, the latter a congenital cranial dysinnervation disorder resulting from heterozygous missense mutations in *KIF21A*.

Low Frequency of A Pattern Strabismus

We have noted frequent A pattern strabismus in DURS2[11] and CFEOM1[24] and have attributed this to LR misinnervation by a CN3 branch normally destined for the IR. In the present family with six DRRS subjects, only one had A pattern and one V pattern strabismus, and only the latter underwent MRI. Although it was impossible to demonstrate directly the innervation to every EOM in DRRS, the relative infrequency of pattern strabismus suggested less frequent motor nerve misrouting to EOMs than in CFEOM1 and DURS2.

Absence of CN3 Hypoplasia

Although the MRI endophenotypes of DURS2 and CFEOM1 feature CN3 hypoplasia, this was not the case for DRRS. Normal CN3 size in DRRS suggested that *SALL4* was not involved in CN3 development or maintenance. It also suggested that anomalous targeting of CN3 axons to the LR did not necessarily result in CN3 hypoplasia.

Absence of Widespread Structural Abnormalities or Hypoplasia of Extraocular Muscles

The only EOM structural abnormalities detected in DRRS were subtle splitting and hypoplasia limited to the deepest portion of the LR muscles in one subject. Only the inferior oblique muscle differed from controls in size; it was slightly smaller in two subjects and slightly larger in one subject. This is in marked contrast to the endophenotypes of DURS2[11] and CFEOM1,[24] in which we reported severe structural abnormalities and hypoplasia of EOMs. In DURS2, the LR often exhibits a striking longitudinal fissure and deep hypoplasia and disorganization,[11] and the SR and SO can be hypoplastic. It has been hypothesized that structural abnormalities of the LR in DURS2 reflect intramuscular innervation abnormalities[11] presumably absent in DRRS. In CFEOM1, the rectus and oblique EOMs exhibit variable to profound hypoplasia, with occasionally severe dysplasia and occasional accessory EOM slips.[24] Thus, although CN6 hypoplasia and aberrant LR innervation by a CN3 branch appear to be features common to all three of these congenital cranial dysinnervation disorders (CCDDs), the endophenotypic abnormalities of DURS2 and CFEOM1 are more widespread than in DRRS.

Absence of Optic Nerve Involvement

Quantitative MRI is useful for ON analysis[27] and has been applied to the CCDDs. In DURS2, ON cross-sections are reduced approximately 25% from normal.[11] In CFEOM1, because of the *KIF21A* mutation, ON cross-sections are reduced 30% to 40% from normal.[24] In contrast, ON size is normal in DRRS, suggesting that *SALL4* is not involved in ON development or maintenance.

Absence of Widespread Pulley Abnormalities

Pulley disorders are associated with some forms of strabismus.[18,32] Rectus EOM path abnormalities are associated with misplaced pulleys in craniosynostosis syndromes caused by mutations in *FGFR*[33] in which orbital nerves and EOM volumes are normal. This contrasted with generally normal pulley positions in our subjects with DRRS and in subjects with in DURS2[11] and CFEOM1.[24] Normal pulley positions, despite abnormal innervation, support the idea that pulley abnormalities may be primary in some persons with strabismus.[21,34,35] *SALL4* is apparently not involved in pulley development.

Vertical Saccade Initiation Failure

Subject 4 exhibited a deficit of visually evoked vertical saccades despite preservation of the vertical vestibulo-ocular reflex. This represented vertical saccade initiation failure, historically termed oculomotor apraxia, and is a central finding associated with metabolic disease and structural lesions of the cortex, brain stem, and cerebellum.[36] Vertical saccade initiation failure was absent in the other subjects with DRRS studied here and, to our knowledge, has not been reported in association with DRS.

Conclusions

DRRS resulting from a relatively selective heterozygous *SALL4* mutation is a CCDD affecting primarily CN6, with secondary misrouting of the inferior division of CN3 to normal or only mildly dysplastic EOMs. These ocular motor manifestations are associated with abnormalities of the radial bone, artery, and associated skeletal musculature. DRRS is not associated with ON abnormality, or widespread abnormalities affecting other ocular motor cranial nerves. The DRRS endophenotype is distinct from DURS2 and CFEOM1, presumably reflecting distinct molecular pathology.

References

1. Duane A. Congenital deficiency of abduction associated with impairment of adduction, retraction movements, contraction of the palpebral fissure and oblique movements of the eye. *Arch Ophthalmol*. 1905;34:133–159.
2. DeRespinis PA, Caputo AR, Wagner RS, Guo S. Duane's retraction syndrome. *Surv Ophthalmol*. 1993;38:257–288.
3. Huber A. Electrophysiology of the retraction syndromes. *Br J Ophthalmol*. 1974;58:293–300.
4. Strachan IM, Brown BH. Electromyography of extraocular muscles in Duane's syndrome. *Br J Ophthalmol*. 1972;56:594–599.
5. Miller NR, Kiel SM, Green WR, Clark AW. Unilateral Duane's retraction syndrome (type 1). *Arch Ophthalmol*. 1982;100:1468–1472.
6. Hotchkiss MG, Miller NR, Clark AW, Green WM. Bilateral Duane's retraction syndrome: a clinical-pathologic case report. *Arch Ophthalmol*. 1980;98:870–874.
7. Parsa CF, Grant E, Dillon WP, du Lac S, Hoyt WF. Absence of the abducens nerve in Duane syndrome verified by magnetic resonance imaging. *Am J Ophthalmol*. 1998;125:399–401.
8. Ozkurt H, Basak M, Oral Y, Ozkurt Y. Magnetic resonance imaging in Duane's retraction syndrome. *J Pediatr Ophthalmol Strabismus*. 2003;40:19–22.
9. Kim JH, Hwang J-M. Hypoplastic oculomotor nerve and absent abducens nerve in congenital fibrosis syndrome and synergistic divergence with magnetic resonance imaging. *Ophthalmology*. 2005;112:728–732.
10. Kim JH, Hwang JM. Presence of abducens nerve according to the type of Duane's retraction syndrome. *Ophthalmology*. 2005;112:109–113.
11. Demer JL, Clark RA, Lim KH, Engle EC. Magnetic resonance imaging evidence for widespread orbital dysinnervation in dominant Duane's retraction syndrome linked to the DURS2 locus. *Invest Ophthalmol Vis Sci*. 2007;48:194–202.
12. Appukuttan B, Gillanders E, Juo SH, et al. Localization of a gene for Duane retraction syndrome to chromosome 2q31. *Am J Hum Genet*. 1999;65:1639–1646.
13. Engle EC, Andrews C, Law K, Demer JL. Two pedigrees segregating Duane's retraction syndrome as a dominant trait linked to the DURS2 genetic locus. *Invest Ophthalmol Vis Sci*. 2007;48:189–193.
14. Evans JC, Frayling TM, Ellard S, Gutowski NJ. Confirmation of linkage of Duane's syndrome and refinement of the disease locus to an 8.8-cM interval on chromosome 2q31. *Hum Genet*. 2000;106:636–638.
15. Al-Baradie R, Yamada K, St Hilaire C, et al. Duane radial ray syndrome (Okihiro syndrome) maps to 20q13 and results from

mutations in SALL4, a new member of the SAL family. *Am J Hum Genet*. 2002;71:1195–1199.
16. Kohlhase J, Heinrich M, Schubert L, et al. Okihiro syndrome is caused by SALL4 mutations. *Hum Mol Genet*. 2002;11:2979–2987.
17. Wabbels BL, Lorenz B, Kohlhause J. No evidence of SALL4-mutations in isolated sporadic Duane retraction "syndrome" (DURS). *Am J Hum Genet*. 2004;131A:216–218.
18. Demer JL. A 12 year, prospective study of extraocular muscle imaging in complex strabismus. *J AAPOS*. 2003;6:337–47.
19. Demer JL, Miller JM. Orbital imaging in strabismus surgery. In: Rosenbaum AL, Santiago AP, eds. *Clinical Strabismus Management: Principles and Techniques*. Philadelphia: WB Saunders; 1999:84–98.
20. Clark RA, Miller JM, Demer JL. Three-dimensional location of human rectus pulleys by path inflections in secondary gaze positions. *Invest Ophthalmol Vis Sci*. 2000;41:3787–3797.
21. Clark RA, Miller JM, Demer JL. Displacement of the medial rectus pulley in superior oblique palsy. *Invest Ophthalmol Vis Sci*. 1998; 39:207–212.
22. Clark RA, Miller JM, Demer JL. Location and stability of rectus muscle pulleys inferred from muscle paths. *Invest Ophthalmol Vis Sci*. 1997;38:227–240.
23. Seitz J, Held P, Strotzer M, et al. MR imaging of cranial nerve lesions using six different high-resolution T1 and T2(*)-weighted 3D and 2D sequences. *Acta Radiol*. 2002;43:349–353.
24. Demer JL, Clark RA, Engle EC. Magnetic resonance imaging evidence for widespread orbital dysinnervation in congenital fibrosis of extraocular muscles due to mutations in KIF21A. *Invest Ophthalmol Vis Sci*. 2005;46:530–539.
25. Kono R, Clark RA, Demer JL. Active pulleys: magnetic resonance imaging of rectus muscle paths in tertiary gazes. *Invest Ophthalmol Vis Sci*. 2002;43:2179–2188.
26. Demer JL, Oh SY, Clark RA, Poukens V. Evidence for a pulley of the inferior oblique muscle. *Invest Ophthalmol Vis Sci*. 2003;44: 3856–3865.
27. Karim S, Clark RA, Poukens V, Demer JL. Quantitative magnetic resonance imaging and histology demonstrates systematic variation in human intraorbital optic nerve size. *Invest Ophthalmol Vis Sci*. 2004;45:1047–1051.
28. von Noorden GK. *Binocular vision and ocular motility: Theory and management of strabismus*. St. Louis: Mosby; 1996.
29. Lim KH, Engle EC, Demer JL. Abnormalities of the oculomotor nerve in congenital fibrosis of the extraocular muscles and congenital oculomotor palsy. *Invest Ophthalmol Vis Sci*. 2007;48:1601–1606.
30. Sato S. Electromyographic study on retraction syndrome. *Jpn J Ophthalmol*. 1960;4:57–66.
31. Kim JH, Hwang J-M. Usefulness of MR imaging in children without characteristic clinical findings of Duane's retraction syndrome. *Am J Neuroradiol*. 2005;26:702–705.
32. Oh SY, Clark RA, Velez F, Rosenbaum AL, Demer JL. Incomitant strabismus associated with instability of rectus pulleys. *Invest Ophthalmol Vis Sci*. 2002;43:2169–2178.
33. Muller U, Steinberger D, Kunze S. Molecular genetics of craniosynostotic syndromes. *Graefes Arch Clin Exp Ophthalmol*. 1997; 235:545–550.
34. Clark RA, Miller JM, Rosenbaum AL, Demer JL. Heterotopic muscle pulleys or oblique muscle dysfunction? *J AAPOS*. 1998;2:17–25.
35. Demer JL, Clark RA, Miller JM. Heterotopy of extraocular muscle pulleys causes incomitant strabismus. In: Lennerstrand G, ed. *Advances in Strabismology*. Buren (Netherlands): Aeolus Press; 1999:91–94.
36. Garbutt S, Harris CM. Abnormal vertical optokinetic nystagmus in infants and children. *Br J Ophthalmol*. 2000;84:451–455.